

# Temporal Interferometry: A Mechanism for Controlling Qubit Transitions During Twisted Rapid Passage with Possible Application to Quantum Computing

Frank Gaitan<sup>\*</sup>

*Department of Physics; Southern Illinois University; Carbondale, IL 62901-4401*

(Dated: January 29, 2003)

## Abstract

In an adiabatic rapid passage experiment, the Bloch vector of a two-level system (qubit) is inverted by slowly inverting an external field to which it is coupled, and along which it is initially aligned. In twisted rapid passage, the external field is allowed to twist around its initial direction with azimuthal angle  $\phi(t)$  at the same time that it is inverted. For polynomial twist:  $\phi(t) \sim Bt^n$ . We show that for  $n \geq 3$ , multiple avoided crossings can occur during the inversion of the external field, and that these crossings give rise to strong interference effects in the qubit transition probability. The transition probability is found to be a rapidly varying function of the twist strength  $B$ , which can be used to control the time-separation of the avoided crossings, and hence the character of the interference. Constructive and destructive interference are possible, and can alter the transition probability by as much as 5-7 orders of magnitude, even at *non-adiabatic* inversion rates. The interference effects are analogous to multi-slit interference with the avoided crossings corresponding to the slits, and the time separating the avoided crossings to the slit spacing. From this perspective, twisted rapid passage with adjustable twist strength acts like a temporal interferometer which allows one to greatly enhance or suppress qubit transitions. Possible application of this interference mechanism to construction of *fast fault-tolerant* quantum CNOT and NOT gates is discussed.

PACS numbers: 03.67.Lx; 07.60.Ly; 31.50.Gh

---

<sup>\*</sup>Electronic address: [gaitan@physics.siu.edu](mailto:gaitan@physics.siu.edu)

## I. INTRODUCTION

Adiabatic rapid passage (ARP) is a well-known procedure for inverting the Bloch vector of a two-level system (qubit) [1]. This is accomplished by inverting an external field  $\mathbf{F}(t)$  which couples to the qubit, and along which the qubit is initially aligned. The field inversion is done on a time-scale that is large compared to the inverse Rabi frequency  $\omega_0^{-1}$  (viz. adiabatic), though small compared to the thermal relaxation time  $\tau$  (viz. rapid). In the usual case,  $\mathbf{F}(t)$  remains within a plane that includes the origin:  $\mathbf{F}(t) = b\hat{\mathbf{x}} + at\hat{\mathbf{z}}$ , with  $-T_0/2 < t < T_0/2$ , and  $\omega_0^{-1} \ll T_0 \ll \tau$ . One can show that ARP can be used to implement a NOT-operation on a qubit, although an adiabatic inversion rate is necessary to maintain a low (per-operation) error probability.

Subsequently [2], Berry introduced the idea of twisted adiabatic rapid passage in which the external field is allowed to twist around its initial direction with azimuthal angle  $\phi(t)$  at the same time that it is adiabatically inverted:  $\mathbf{F}(t) = b\cos\phi(t)\hat{\mathbf{x}} + b\sin\phi(t)\hat{\mathbf{y}} + at\hat{\mathbf{z}}$ . Reference 2 showed that the exponentially small transition probability contains a factor  $\exp[\Gamma_g]$  of purely geometric origin. The simplest case where  $\Gamma_g \neq 0$  corresponds to quadratic twist:  $\phi(t) = Bt^2$ . Zwanziger et. al. [3] were able to experimentally realize ARP with quadratic twist and obtained results in accordance with Berry's theory.

In this paper we will consider rapid passage with polynomial twist,  $\phi(t) \sim Bt^n$ , and will remove the restriction of inversion at adiabatic rates. Our interest will not be the geometric effect of Reference 2, although we will briefly consider quadratic twist in Section II as a test case for our numerical simulations. Instead, our focus will be on the occurrence of multiple avoided crossings during twisted rapid passage when  $n \geq 3$ . After general considerations (Section II), we will explicitly examine cubic ( $n = 3$ ) and quartic ( $n = 4$ ) twist, and will provide clear evidence that the multiple avoided crossings produce strong interference effects in the qubit transition probability. The transition probability is shown to be a rapidly varying function of the twist strength  $B$ , which can be used to control the time-separation of the avoided crossings, and hence the character of the interference (constructive or destructive). Cubic and quartic twist are examined in Sections III and IV, respectively. We shall see that interference between the multiple avoided crossings can greatly enhance or suppress qubit transitions, and that for quartic twist, suppression of the transition probability by 5-7 orders of magnitude is possible, even at *non-adiabatic* inversion rates. These interference effects are analogous to multi-slit interference with the avoided crossings corresponding to the slits, and the time-separating the avoided crossings to the slit spacing. From this perspective, twisted rapid passage with adjustable twist strength acts like a temporal interferometer through which one can greatly enhance or suppress qubit transitions. Finally, in Section V, we summarize our results and discuss possible application of this interference mechanism to quantum computing.

## II. TWISTED RAPID PASSAGE

We begin by briefly summarizing the essential features of rapid passage in the absence of twist. Twistless rapid passage describes a wide variety of phenomena, ranging from magnetization reversal in NMR, to electronic transition during a slow atomic collision. The

essential situation is that of a qubit which is Zeeman-coupled to a background field  $\mathbf{F}(t)$ ,

$$H(t) = \boldsymbol{\sigma} \cdot \mathbf{F}(t) = \begin{pmatrix} at & b \\ b & -at \end{pmatrix} , \quad (1)$$

with  $\mathbf{F}(t) = b \hat{\mathbf{x}} + at \hat{\mathbf{z}}$ . This particular form for  $\mathbf{F}(t)$  describes inversion of the background field in such a way that it remains in the x-z plane throughout the inversion. For simplicity, we assume  $a, b > 0$  throughout this paper. The instantaneous energies  $E_{\pm}(t)$  are:

$$E_{\pm}(t) = \pm \sqrt{b^2 + (at)^2} , \quad (2)$$

and an avoided crossing is seen to occur at  $t = 0$  where the energy gap is minimum. The Schrodinger dynamics for twistless rapid passage can be solved exactly for arbitrary values of  $a$  and  $b$  [4, 5], and yields the Landau-Zener expression for the transition probability  $P_{LZ}$ :

$$P_{LZ} = \exp \left[ -\frac{\pi b^2}{\hbar |a|} \right] . \quad (3)$$

In *twisted* rapid passage, the background field  $\mathbf{F}(t)$  is allowed to twist around its initial direction during the course of its inversion:  $\mathbf{F}(t) = b \cos \phi(t) \hat{\mathbf{x}} + b \sin \phi(t) \hat{\mathbf{y}} + at \hat{\mathbf{z}}$ . It proves convenient to transform to the rotating frame in which the x-y component of the background field is instantaneously at rest. This is accomplished via the unitary transformation  $U(t) = \exp[-(i/2)\phi(t)\sigma_z]$ . The Hamiltonian  $\overline{H}(t)$  in this frame is:

$$\overline{H}(t) = \boldsymbol{\sigma} \cdot \overline{\mathbf{F}} = \begin{pmatrix} \left( at - \frac{\hbar \dot{\phi}}{2} \right) & b \\ b & - \left( at - \frac{\hbar \dot{\phi}}{2} \right) \end{pmatrix} , \quad (4)$$

where  $\overline{\mathbf{F}}(t) = b \hat{\mathbf{x}} + (at - \hbar \dot{\phi}/2) \hat{\mathbf{z}}$  is the background field as seen in the rotating frame, and a dot over a symbol represents the time derivative of that symbol. The instantaneous energy eigenvalues are  $\overline{E}_{\pm}(t) = \pm \sqrt{\left( at - (\hbar \dot{\phi})/2 \right)^2 + b^2}$ . Avoided crossings occur when the energy gap is minimum, corresponding to when

$$at - \frac{\hbar}{2} \frac{d\phi}{dt} = 0 . \quad (5)$$

For polynomial twist:  $\phi_n(t) = c_n B t^n$ , where  $B$  is the twist strength. The dimensionless constant  $c_n$  has been introduced to simplify some of the formulas below. For later convenience, we chose  $c_n = 2/n$ . For polynomial twist, it is easily checked that eqn. (5) always has the root:

$$t = 0 , \quad (6)$$

and that for  $n \geq 3$ , eqn. (5) also has the  $n - 2$  roots:

$$t = (\text{sgn } B)^{\frac{1}{n-2}} \left( \frac{a}{\hbar |B|} \right)^{\frac{1}{n-2}} . \quad (7)$$

All together, equation (5) has  $n - 1$  roots, though only the real roots correspond to avoided crossings. For quadratic twist ( $n = 2$ ), only eqn. (6) arises. Thus, for this case, only the

TABLE I: Classification of regimes under which multiple avoided crossings occur for polynomial twist with  $n \geq 3$ .

1. $\text{sgn } B = +1$			
(a)	$n$ odd;	2 avoided crossings at:	$t = 0$ and $t = (a/\hbar B)^{1/(n-2)}$
(b)	$n$ even;	3 avoided crossings at:	$t = 0$ and $t = \pm (a/\hbar B)^{1/(n-2)}$
2. $\text{sgn } B = -1$			
(a)	$n$ odd;	2 avoided crossings at:	$t = 0$ and $t = -(a/\hbar  B )^{1/(n-2)}$
(b)	$n$ even;	1 avoided crossing at:	$t = 0$

avoided crossing at  $t = 0$  is possible. For  $n \geq 3$ , along with the avoided crossing at  $t = 0$ , real solutions to eqn. (7) also occur. The different possibilities for this situation are summarized in Table I. We see that for polynomial twist with  $n \geq 3$ , multiple avoided crossings always occur for positive twist strength  $B$ , while for negative twist strength, multiple avoided crossings only occur when  $n$  is odd. Note that the time separating the multiple avoided crossings can be adjusted by variation of the twist strength  $B$  and/or the inversion rate  $a$ .

As mentioned earlier, quadratic twist has already been examined in the literature [2]. It is of interest here only because its dynamics can be solved exactly, and thus allows us to test our numerical simulations before proceeding to unexplored cases of twisted rapid passage. For quadratic twist,  $\dot{\phi}_2 = 2Bt$ . Inserting this into eqn. (4) gives  $\bar{\mathbf{F}}(t) = b\hat{\mathbf{x}} + \bar{a}t\hat{\mathbf{z}}$ , with  $\bar{a} = a - \hbar|B|(\text{sgn } B)$ . Thus rapid passage with quadratic twist maps onto twistless rapid passage with  $a \rightarrow \bar{a}$ . This allows us to obtain an exact result for the transition probability  $P_2$  for arbitrary values of  $a$  and  $b$  from eqn. (3) with  $a \rightarrow \bar{a}$ :

$$P_2 = \exp \left[ -\frac{\pi b^2}{\hbar |a - \hbar|B|(\text{sgn } B)|} \right] . \quad (8)$$

In the adiabatic limit, this reduces to  $P_2 = P_{LZ} \exp[\Gamma_g]$ , where  $\Gamma_g = -\pi B b^2/a^2$  is the geometric exponent discovered in Ref. [2]. Eqn. (8) makes the interesting prediction that a *complete* quenching of transitions will occur when  $\text{sgn } B = +1$  and  $a = \hbar B$ , while no such quenching is possible for  $\text{sgn } B = -1$ . Zwanziger et. al. [3] were able to realize rapid passage with quadratic twist experimentally and confirmed the existence of  $\Gamma_g$ , and the twist-dependent quenching of transitions. We now show that our numerical simulation also reproduces these effects.

The equations that drive the numerical simulation follow from the Schrodinger equation in the non-rotating frame:

$$i\hbar \frac{\partial}{\partial t} |\psi\rangle = H(t) |\psi\rangle , \quad (9)$$

where  $H(t) = \boldsymbol{\sigma} \cdot \mathbf{F}(t)$ , and  $\mathbf{F}(t) = b \cos \phi(t) \hat{\mathbf{x}} + b \sin \phi(t) \hat{\mathbf{y}} + at \hat{\mathbf{z}}$ . To obtain these equations in the adiabatic representation, we expand  $|\psi(t)\rangle$  in the instantaneous eigenstates  $|E_{\pm}(t)\rangle$  of  $H(t)$ :

$$|\psi(t)\rangle = S(t) e^{-\frac{i}{\hbar} \int_{-T_0/2}^t d\theta (E_- - \hbar \dot{\gamma}_-)} |E_-(t)\rangle - I(t) e^{-\frac{i}{\hbar} \int_{-T_0/2}^t d\theta (E_+ - \hbar \dot{\gamma}_+)} |E_+(t)\rangle . \quad (10)$$

Here  $\gamma_{\pm}(t)$  are the Berry phases [6] associated with the energy-levels  $E_{\pm}(t)$ , respectively, and

$$\dot{\gamma}_{\pm}(t) = i \langle E_{\pm}(t) | \frac{d}{dt} | E_{\pm}(t) \rangle = i \langle E_{\pm}(t) | \dot{E}_{\pm}(t) \rangle . \quad (11)$$

Substituting eqn. (10) into (9), and using the orthonormality of the instantaneous eigenstates, one obtains the equations of motion for the expansion coefficients  $S(t)$  and  $I(t)$ :

$$\frac{dS}{dt} = -\Gamma^*(t) e^{-i \int_{-T_0/2}^t d\theta \delta(\theta)} I(t) , \quad (12a)$$

$$\frac{dI}{dt} = \Gamma(t) e^{i \int_{-T_0/2}^t d\theta \delta(\theta)} S(t) . \quad (12b)$$

Here,

$$\delta(t) = \frac{E_+(t) - E_-(t)}{\hbar} - (\dot{\gamma}_+(t) - \dot{\gamma}_-(t)) , \quad (13)$$

$$\Gamma(t) = \langle E_+(t) | \dot{E}_-(t) \rangle , \quad (14)$$

and one can show that  $\Gamma^*(t) = -\langle E_-(t) | \dot{E}_+(t) \rangle$ . Eqns. (12) are the qubit equations of motion in the adiabatic representation and include the influence of Berry's phase on the dynamics through  $\delta(t)$ . In the case of twistless rapid passage, Berry's phase vanishes, and eqns. (12) reduce to the well-known equations of motion for a two-level system found in Ref. [7]. Eqns. (12) can be put in dimensionless form if we introduce the dimensionless variables:  $\tau = (a/b)t$ ,  $\bar{\Gamma} = (b/a)\Gamma$ , and  $\bar{\delta} = (b/a)\delta$ . Here  $a$  and  $b$  are the parameters that appear in the background field  $\mathbf{F}(t)$ . One obtains:

$$\frac{dS}{d\tau} = -\bar{\Gamma}^* e^{-i \int_{-\tau_0/2}^{\tau} d\theta \bar{\delta}(\theta)} I(\tau) , \quad (15a)$$

$$\frac{dI}{d\tau} = \bar{\Gamma} e^{i \int_{-\tau_0/2}^{\tau} d\theta \bar{\delta}(\theta)} S(\tau) , \quad (15b)$$

where  $\tau_0 = (a/b)T_0$  is the (dimensionless) time over which the qubit evolves. For rapid passage, the qubit is initially in the negative energy level  $|E_-(-\tau_0/2)\rangle$ . This corresponds to the initial condition:

$$S(-\tau_0/2) = 1 , \quad (16a)$$

$$I(-\tau_0/2) = 0 . \quad (16b)$$

Our numerical simulation integrates eqns. (15) over the time-interval  $[-\tau_0/2, \tau_0/2]$  subject to initial condition (16). From this we determine the asymptotic transition probability  $P$ :

$$P = |I(\tau_0/2)|^2 , \quad (17)$$

for  $\tau_0 \gg 1$ . Later, we will need the  $\tau$ -values corresponding to the avoided crossings. These are determined by rewriting eqns. (6) and (7) in dimensionless form. To this end, we introduce

$$\eta_n = \frac{\hbar B b^{n-2}}{a^{n-1}} , \quad (18)$$

and recalling that  $\tau = (a/b)t$ , one easily obtains:

$$\tau = 0 , \quad (19)$$

and

$$\tau = (\text{sgn } \eta_n)^{\frac{1}{n-2}} \left[ \frac{1}{|\eta_n|} \right]^{\frac{1}{n-2}} . \quad (20)$$

The avoided crossings correspond to  $\tau = 0$  and also, for  $n \geq 3$ , the real solutions of eqn. (20).

For quadratic twist  $\phi_2(t) = Bt^2$ . The instantaneous eigenvalues and eigenvectors of  $H(t)$  are easily found to be  $E_{\pm}(t) = \pm E(t)$ , where  $E(t) = \sqrt{b^2 + (at)^2}$ , and

$$|E_+(t)\rangle = \begin{pmatrix} \cos \frac{\theta}{2} \\ \sin \frac{\theta}{2} e^{i\phi_2} \end{pmatrix} ; \quad |E_-(t)\rangle = \begin{pmatrix} \sin \frac{\theta}{2} \\ -\cos \frac{\theta}{2} e^{i\phi_2} \end{pmatrix} , \quad (21)$$

with  $\cos \theta = at/E$ . From the eigenstates one obtains:

$$\dot{\gamma}_{\pm}(t) = -\frac{\dot{\phi}_2}{2} (1 \mp \cos \theta) ; \quad (22a)$$

$$\Gamma(t) = \frac{\dot{\theta}}{2} - i \frac{\dot{\phi}_2}{2} \sin \theta ; \quad (22b)$$

$$\delta(t) = \frac{2E}{\hbar} - \dot{\phi}_2 \cos \theta . \quad (22c)$$

$\bar{\Gamma}(\tau)$  and  $\bar{\delta}(\tau)$  are then determined from eqns. (22b) and (22c) and are found to depend parametrically on the dimensionless “inversion rate”  $\lambda = \hbar a/b^2$  and the dimensionless “twist strength”  $\eta_2 = \hbar B/a$ . “Inversion rate” and “twist strength” are placed in quotes as  $\lambda$  does not depend solely on the inversion rate  $a$ , nor  $\eta_2$  solely on the twist strength  $B$ . Crudely speaking,  $\lambda = 1$  can be thought of as the boundary separating adiabatic and non-adiabatic inversion rates, with  $\lambda > 1$  corresponding to non-adiabatic inversion. Having determined  $\bar{\Gamma}(\tau)$  and  $\bar{\delta}(\tau)$ , eqns. (15) are integrated numerically using an adjustable step-size fourth-order Runge-Kutta algorithm. To simplify comparison of the numerical result for the transition probability with the exact result  $P_2$ , we re-write eqn. (8) in terms of  $\lambda$  and  $\eta_2$ . One finds:

$$P_2 = \exp \left[ -\frac{\pi}{\lambda} \frac{1}{|1 - \eta_2|} \right] . \quad (23)$$

Figure 1 shows a representative plot of the transition probability  $P(\tau) = |I(\tau)|^2$  versus  $\tau$ . It is clear for the Figure that the transition occurs in the vicinity of the avoided crossing at  $\tau = 0$ . Note also that  $P(\tau)$  has a small oscillation about its asymptotic value  $P = \lim_{\tau \rightarrow \infty} P(\tau)$ . To average out the oscillation,  $P(\tau)$  (for given  $\lambda$  and  $\eta_2$ ) was calculated for 10 different values of  $\tau \gg 1$ , and  $P$  was identified with the average [8]. Figures 2 and 3 show our numerical results for  $P$  for various values of  $\eta_2$  for  $\lambda = 10.0$  and  $\lambda = 3.0$ , respectively. Also plotted in each of these Figures is the exact result  $P_2$  (eqn. (23)). Figures 2 and 3 show that our numerical results are in excellent agreement with the exact result  $P_2$ , and clearly show the quenching of transitions at  $\eta_2 = 1$ , and the absence of quenching for negative  $\eta_2$ . The  $\lambda$  values shown are purposely highly non-adiabatic. We see that the twist-induced quenching clearly persists into the non-adiabatic regime, although the width of the quench decreases with increasing  $\lambda$ . The agreement of our simulations with eqn. (23) at small  $\eta_2$  indicates that our simulations also account for the geometric factor  $\exp[\Gamma_g]$  in  $P_2$ . Having established

### Transition Probability vs. Time

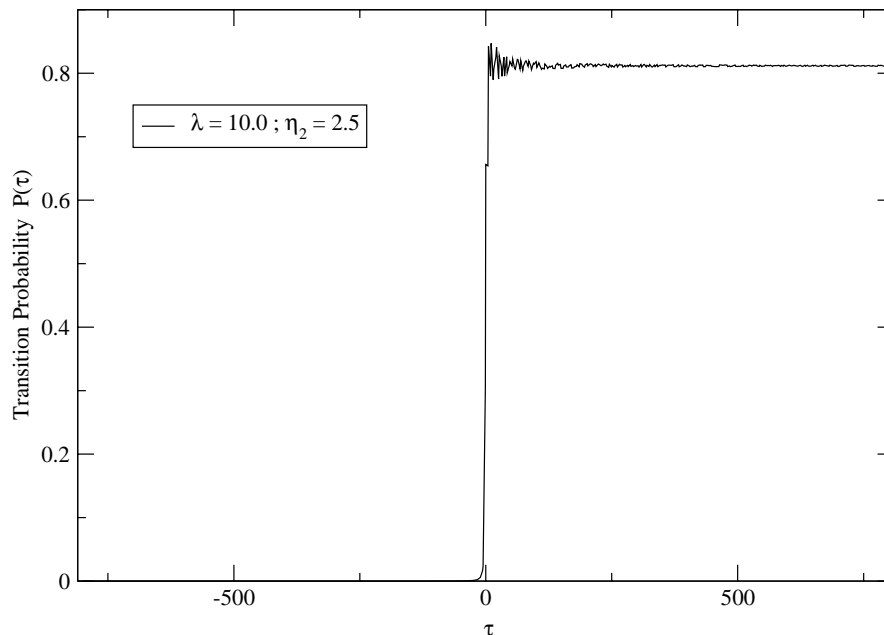


FIG. 1: Representative plot of transition probability  $P(\tau)$  for quadratic twist with  $\lambda = 10.0$  and  $\eta_2 = 2.5$ .

that our numerical algorithm correctly reproduces the essential results of rapid passage with quadratic twist, we go on to consider the unexplored areas of rapid passage with higher order twist. Referring to Table I, we see that all cases with odd  $n$  have 2 avoided crossings. Cubic ( $n = 3$ ) twist corresponds to the simplest example of odd-order twist, and it is examined in the following Section. Similarly, quartic ( $n = 4$ ) twist is the simplest example of even-order twist, and we examine it in Section IV.

### III. CUBIC TWIST

Having successfully tested our numerical algorithm against the exact results for quadratic twist, we go on to consider cubic twist for which  $\phi_3(t) = (2/3)Bt^3$ , and  $\eta_3 = \hbar Bb/a^2$  (see eqn. (18)). As in Section II, the instantaneous eigenvalues of  $H(t)$  are  $E_{\pm}(t) = \pm E(t)$ , and the instantaneous eigenstates are given by eqn. (21) with  $\phi_2(t) \rightarrow \phi_3(t)$ . Eqns. (22) again apply, however  $\dot{\phi}_2(t) \rightarrow \dot{\phi}_3(t)$ , and  $\bar{\Gamma}(\tau)$  and  $\bar{\delta}(\tau)$  are determined from eqns. (22b) and (22c). Having determined  $\bar{\Gamma}(\tau)$  and  $\bar{\delta}(\tau)$ , eqns. (15) can be numerically integrated subject to the initial condition specified in eqns. (16). Before examining results of that integration, we show in Figure 4 a plot of the numerical results for the transition probability  $P(\tau)$  for  $\lambda = 5.0$  and  $\eta_3 = 0$ . This corresponds to twistless non-adiabatic rapid passage, and we include this plot for later comparison with related plots for cubic and quartic twist. The asymptotic transition probability for this case is  $P = 0.533$ . Thus, if we were to use this example of twistless non-adiabatic rapid passage to implement a fast NOT-operation on a qubit, the operation would be slightly more likely to produce a bit-flip error than not. We will show below that if a small amount of cubic twist is included, the bit-flip error probability can be

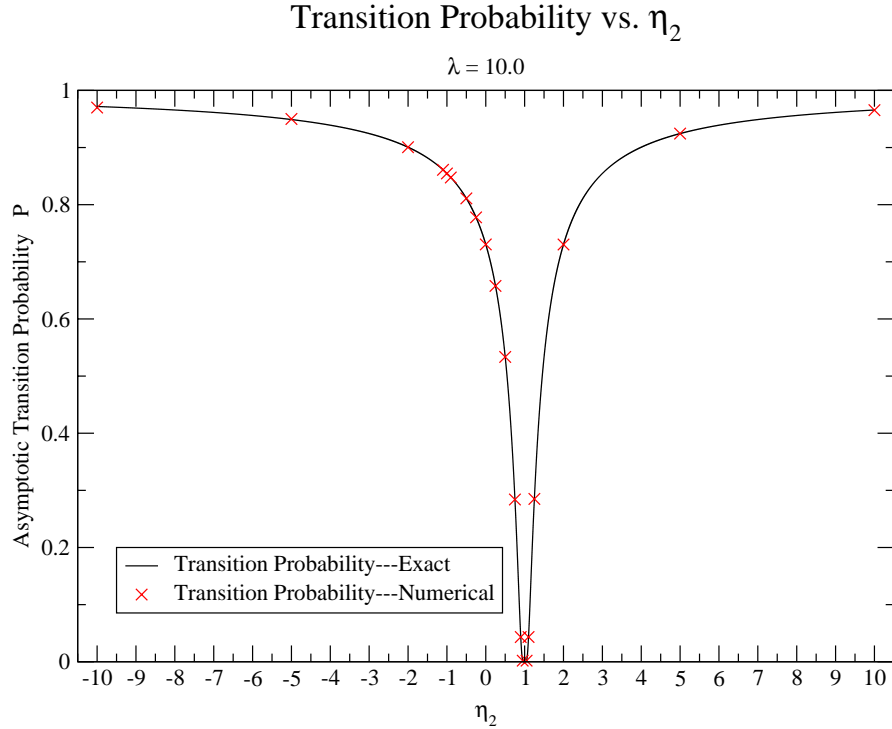


FIG. 2: Numerical results for the asymptotic transition probability  $P$  versus  $\eta_2$  for quadratic twist with  $\lambda = 10.0$ . Also plotted is the exact result  $P_2$ .

reduced by 2 orders of magnitude while still maintaining the non-adiabatic inversion rate  $\lambda = 5.0$ . This substantial reduction in error probability is due to destructive interference between the two avoided crossings that occur during rapid passage with cubic twist.

From eqns. (19) and (20), we see that cubic twist is expected to have 2 avoided crossings at  $\tau_1 = 0$  and  $\tau_2 = \text{sgn } \eta_3 / |\eta_3|$ . Figures 5 and 6 show  $P(\tau)$  for  $\lambda = 5.0$  and  $\eta_3 = 0.02$  and  $\eta_3 = -0.02$ , respectively. Figure 5 (6) clearly shows the expected avoided crossings at  $\tau = 0$  and  $\tau = 50$  ( $-50$ ). It is also clear from these Figures, and comparison with Figure 4, that the avoided crossings are constructively interfering, leading to an asymptotic transition probability of  $P = 0.997$ . Figures 7 and 8 show  $P(\tau)$  for  $\lambda = 5.0$  and  $\eta_3 = 0.05$  and  $-0.05$ , respectively. The avoided crossings in Figure 7 (8) clearly occur at  $\tau = 0$  and  $\tau = 20$  ( $-20$ ) as expected. Here the avoided crossings interfere destructively, with  $P = 0.270$ . Summarizing, we see that: (1) two avoided crossings do occur during rapid passage with cubic twist as predicted in Table I; (2) the avoided crossings produce interference effects in the asymptotic transition probability  $P$  which can be controlled through variation of their separation; and (3) the separation of the avoided crossings  $\Delta\tau_{ac} = |\tau_2 - \tau_1| = 1/|\eta_3|$  can be altered by varying  $\eta_3 = \hbar Bb/a^2$ . We now consider two possible applications of this interference effect.

First, consider twistless adiabatic rapid passage with  $\lambda = 0.5$  and  $\eta_3 = 0$ . Figure 9 show the transition probability  $P(\tau)$  for this case. The asymptotic transition probability is  $P = 1.87 \times 10^{-3}$ . Figure 10 shows  $P(\tau)$  for adiabatic rapid passage with cubic twist with  $\lambda = 0.5$  and  $\eta_3 = 0.04$ . The asymptotic transition probability in this case is  $P = 0.996$ ! Thus, by introducing a small amount of cubic twist, constructive interference between the avoided crossings transforms adiabatic rapid passage into a non-resonant pump for the qubit



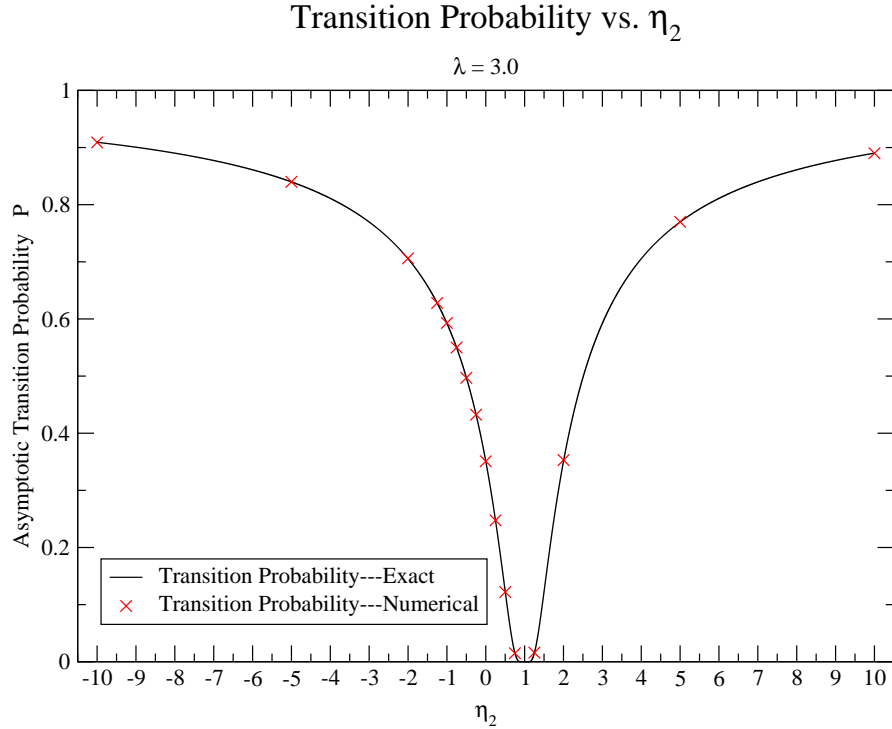


FIG. 3: Numerical results for the asymptotic transition probability  $P$  versus  $\eta_2$  for quadratic twist with  $\lambda = 3.0$ . Also plotted is the exact result  $P_2$ .

energy levels. Figures 5 and 6 indicate that, should it be desired, equally large transition probabilities are also possible at faster inversion rates  $\lambda$ . It is worth pointing out that to produce such a large transition probability using twistless non-adiabatic rapid passage would require  $\lambda = 784$  (see eqn. (23) with  $\eta_2 = 0$ ) as opposed to  $\lambda \sim 0.5 - 5.0$  when cubic twist is exploited.

We now show that one can utilize the interference between avoided crossings to strongly suppress qubit transitions during *non-adiabatic* rapid passage with cubic twist. Figure 11 shows  $P(\tau)$  for  $\lambda = 5.0$  and  $\eta_3 = 4.577 \times 10^{-2}$ . The asymptotic transition probability for this case is  $P = 3.44 \times 10^{-3}$ . This is to be compared with twistless rapid passage with  $\lambda = 5.0$  (Figure 4) for which  $P = 0.533$ . Destructive interference between the two avoided crossings has reduced the transition probability  $P$  by 2 orders of magnitude relative to the twistless case shown in Figure 4. Thus if we were to implement a fast NOT-operation using non-adiabatic rapid passage with cubic twist at  $\lambda = 5.0$  and  $\eta_3 = 4.577 \times 10^{-2}$ , we would obtain (on average) 1 bit-flip error per 291 NOT-operations. By comparison, twistless rapid passage with  $\lambda = 5.0$  would produce (on average) 1 bit-flip error for every 2 NOT-operations. This result strongly suggest the value of exploring whether this destructive interference between avoided crossings during twisted rapid passage could be exploited to produce fast reliable quantum NOT and CNOT logic gates. Our numerical results indicate that  $P$  will lie in the range  $(3.44 \times 10^{-3}, 4.69 \times 10^{-3})$  for  $\eta_3$  lying in the range  $(4.576 \times 10^{-2}, 4.578 \times 10^{-2})$  so that it should be possible to lock on to destructive interference if one can control  $\eta_3$  to 4 significant figures. As striking as this result for cubic twist is, we shall see in the following Section that quartic twist can reduce the bit-flip error probability even more dramatically.

### Transition Probability vs. Time

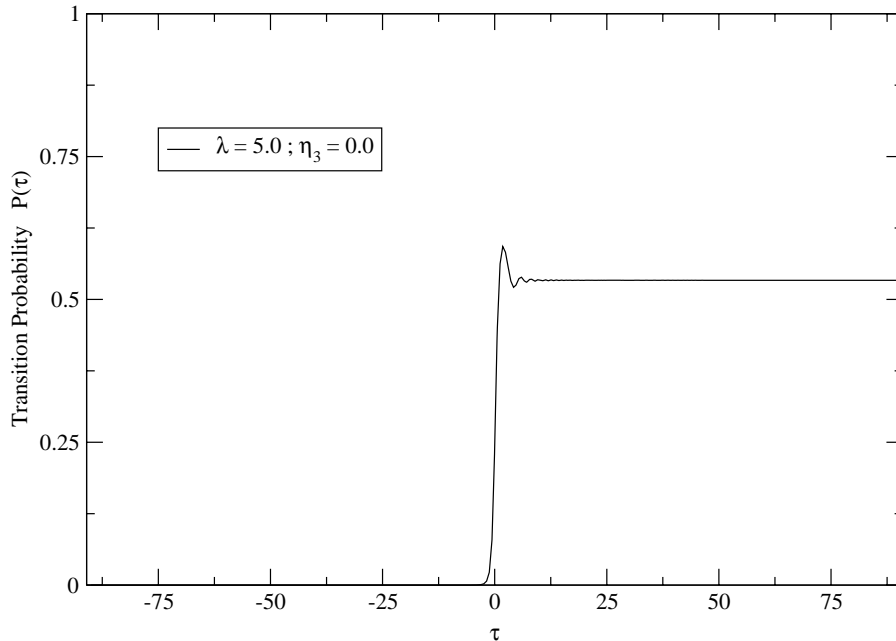


FIG. 4: Plot of the transition probability  $P(\tau)$  for twistless non-adiabatic rapid passage with  $\lambda = 5.0$  and  $\eta_3 = 0$ .

### IV. QUARTIC TWIST

For quartic twist  $\phi_4(t) = (1/2)Bt^4$  and  $\eta_4 = \hbar Bb^2/a^3$ . Avoided crossings are expected to occur at  $\tau_1 = 0$ , and at  $\tau_2 = \pm 1/\sqrt{\eta_4}$  (when  $\text{sgn } \eta_4 = +1$ ; see eqn. (20) and Table I). Formally, the analysis of quartic twist parallels that of quadratic and cubic twist. With the substitution  $\phi_2(t) \rightarrow \phi_4(t)$ , eqns. (21) and (22) continue to apply, and one determines  $\bar{\Gamma}(\tau)$  and  $\bar{\delta}(\tau)$  from eqns. (22b) and (22c). Once  $\bar{\Gamma}(\tau)$  and  $\bar{\delta}(\tau)$  are known, eqns. (15) can be integrated numerically subject to the initial condition specified in eqns. (16).

In Figure 12 we plot the transition probability  $P(\tau)$  for  $\lambda = 5.0$  and  $\eta_4 = 4.6 \times 10^{-4}$ . The expected avoided crossings at  $\tau_1 = 0$  and  $\tau_2 = \pm 46.63$  are clearly visible. The asymptotic transition probability for this case is  $P = 0.88 \pm 0.01$  [8]. For twistless rapid passage with  $\lambda = 5.0$  (see Figure 4),  $P = 0.533$ . Thus the avoided crossings in Figure 12 are constructively interfering, leading to an enhancement of the transition probability  $P$ . Figure 13 shows  $P(\tau)$  for quartic twist with  $\lambda = 5.0$  and  $\eta_4 = -4.6 \times 10^{-4}$ . This Figure clearly shows only one avoided crossing at  $\tau_1 = 0$ , as expected for  $\text{sgn } \eta_4 = -1$  (see Table I). The asymptotic transition probability in this case is  $P = 0.533 \pm 0.001$  which equals the result for twistless rapid passage with  $\lambda = 5.0$  (Figure 4) to the level of precision obtained in our calculation.

Figure 14 plots  $P(\tau)$  for  $\lambda = 5.0$  and  $\eta_4 = 1.6 \times 10^{-3}$ . The Figure clearly shows the expected crossings at  $\tau_1 = 0$  and  $\tau_2 = \pm 25.0$ . The asymptotic transition probability is  $P = 6.93 \times 10^{-4}$  and corresponds to destructive interference relative to twistless rapid passage with  $\lambda = 5.0$  (Figure 4). We do not include a plot of  $P(\tau)$  for  $\lambda = 5.0$  and  $\eta_4 = -1.6 \times 10^{-3}$  as it is similar to Figure 13: one avoided crossing at  $\tau_1 = 0$  and  $P = 0.533 \pm 0.008$ .

Summarizing these results, we see that: (i) three (one) avoided crossings (crossing) occur(s) as predicted in Table I when  $\text{sgn } \eta_4 = +1$  ( $-1$ ); (ii) the avoided crossings produce

### Transition Probability vs. Time

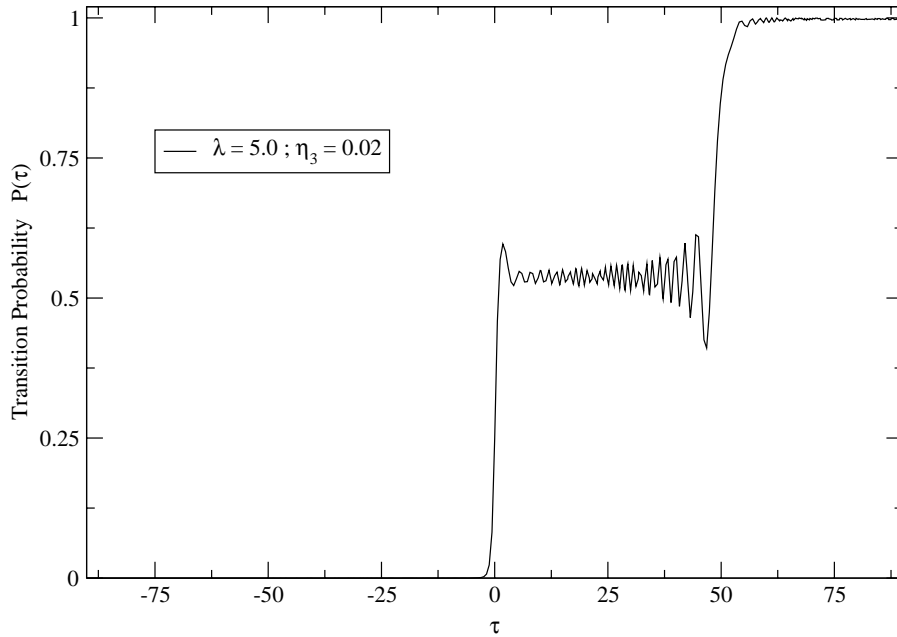


FIG. 5: The transition probability  $P(\tau)$  for non-adiabatic rapid passage with cubic twist with  $\lambda = 5.0$  and  $\eta_3 = 0.02$ .

interference effects in the transition probability, with the character of the interference (constructive or destructive) determined by the separation of the avoided crossings; and (iii) the separation of adjacent avoided crossings is given by  $\Delta\tau_{ac} = |\tau_2 - \tau_1| = 1/\sqrt{\eta_4}$  ( $\text{sgn } \eta_4 = +1$ ), and it is controllable through variation of  $\eta_4 = \hbar B b^2/a^3$ .

Quartic twist does not appear to be as effective at pumping the qubit energy-levels as cubic twist. Figure 15 shows  $P(\tau)$  for  $\lambda = 0.5$  and  $\eta_4 = 6.45 \times 10^{-3}$ . The expected avoided crossings at  $\tau_1 = 0$  and  $\tau_2 = \pm 12.45$  are clearly visible, and the asymptotic transition probability is  $P = 0.20 \pm 0.02$ . Although this is a 2 order of magnitude improvement over twistless adiabatic rapid passage with  $\lambda = 0.5$  (Figure 9), it falls well short of the transition probability  $P = 0.996$  easily obtainable with cubic twist. In fact, for  $\eta_4 < 1$ ,  $P \sim 0.20$  was among the largest  $P$ -values we could find. If larger values of twist strength are allowed, the largest transition probability we could find was  $P = 0.64$  at  $\eta_4 = 3.00$ .

Quartic twist, however, proves to be much more effective at quenching transitions during non-adiabatic rapid passage than cubic twist. Because the asymptotic transition probability  $P$  for quartic twist is found to be a rapidly varying function of the parameters  $(\eta_4, \tau_0, \lambda)$ , the degree to which the enhanced quenching can be realized is limited by how precisely these parameters can be controlled. Suppose that these parameters are known to 5 significant figures, and that we implement a quantum NOT operation using rapid passage with quartic twist. Due to the uncertainty in the 6th digit of these parameters, the asymptotic transition probability  $P$  will vary over a finite range of values. The least upper bound  $\bar{P}$  for this range gives a measure of the worst case error probability for the NOT operation. To estimate the value of this least upper bound,  $P$  was calculated for 30 sets of values of  $(\eta_4, \tau_0, \lambda)$  which to 5 significant figures were all  $(\eta_4 = 4.0031 \times 10^{-3}, \tau_0 = 120.00, \lambda = 5.0000)$ , and which differed only in the 6th digit of each parameter's mantissa. The least upper bound for the range of

### Transition Probability vs. Time

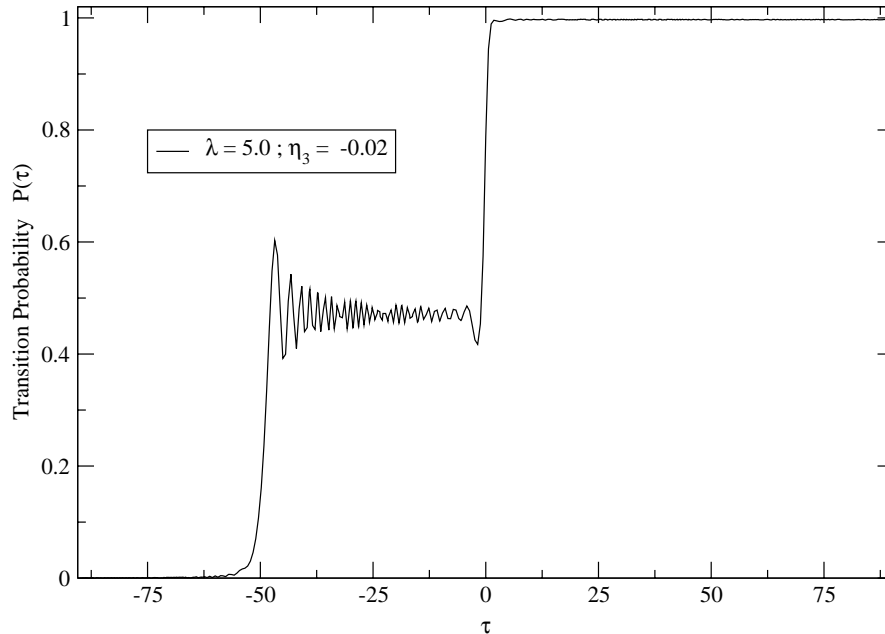


FIG. 6: The transition probability  $P(\tau)$  for non-adiabatic rapid passage with cubic twist with  $\lambda = 5.0$  and  $\eta_3 = -0.02$ .

$P$  values found was  $\overline{P} = 0.632 \times 10^{-5}$ . Repeating this analysis for  $(\eta_4, \tau_0, \lambda)$  known to 6 significant figures gave  $\overline{P} = 0.577 \times 10^{-7}$ , and to 7 significant figures gave  $\overline{P} = 0.616 \times 10^{-9}$ . Thus, if  $(\eta_4, \tau_0, \lambda)$  can be controlled to 5 significant figures, the NOT operation error probability  $\overline{P}$  can be reduced by 5 orders of magnitude relative to twistless rapid passage with  $\lambda = 5.0$  for which  $P = 0.533$ . Controlling  $(\eta_4, \tau_0, \lambda)$  to 6 significant figures yields a 7 order of magnitude reduction in the error probability relative to the twistless case. To put these numbers into perspective, existing estimates of the accuracy threshold  $P_{acc}$  for fault-tolerant operation of a quantum gate [9] give  $P_{acc} \sim 10^{-4} - 10^{-5}$ . Our analysis raises the exciting possibility that non-adiabatic rapid passage with quartic twist might provide a means of realizing *fast fault-tolerant* NOT and CNOT gates. The novelty of this prospect is the marriage of operational speed with fault-tolerance. Adiabatic rapid passage can produce error probabilities below  $P_{acc}$ , though only while operating at adiabatic inversion rates. This marriage of speed and reliability is a direct consequence of the destructive interference which is possible between the 3 avoided crossings that can arise during rapid passage with quartic twist. Because of their ubiquitousness in quantum computing and quantum error correction [10, 11, 12], experimental realization of a fast fault-tolerant quantum CNOT gate would be a significant development in the effort to build a working quantum computer.

## V. DISCUSSION

It has been our aim in this paper to show that multiple avoided crossings can arise during twisted rapid passage, and that by varying their time-separation, interference effects are produced which allow for a direct control over qubit transitions. This time-separation is

### Transition Probability vs. Time

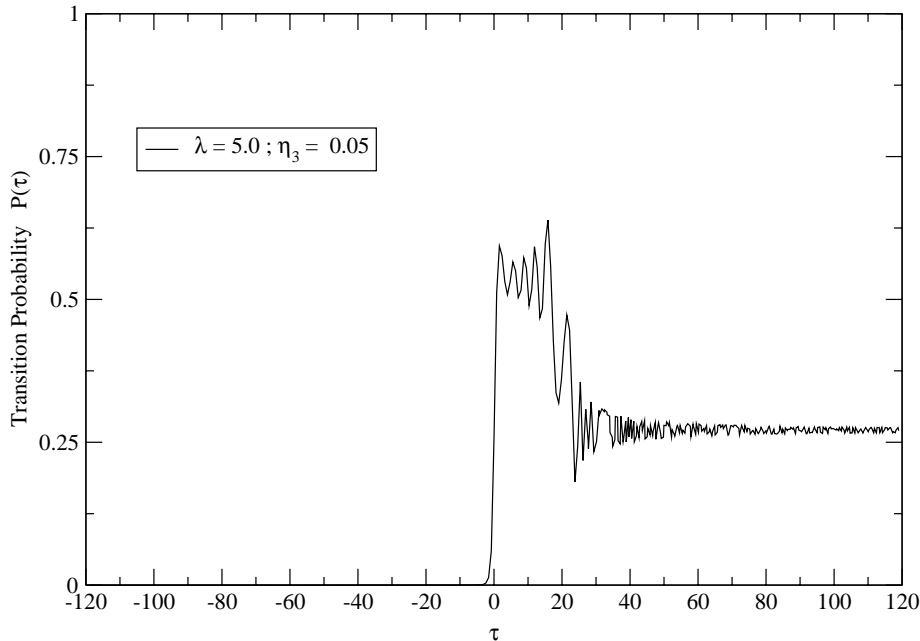


FIG. 7: The transition probability  $P(\tau)$  for non-adiabatic rapid passage with cubic twist with  $\lambda = 5.0$  and  $\eta_3 = 0.05$ .

controlled through the (dimensionless) twist strength  $\eta$ , and the resulting interference can be constructive (enhancing transitions) or destructive (reducing transitions). For  $n$ th-order polynomial twist,  $\eta_n = \hbar B b^{n-2} / a^{n-1}$ , where  $B$  is the (dimensionful) twist strength,  $2b$  is the energy-gap separating the qubit energy-levels at an avoided crossing, and  $a$  is the inversion rate of the external field  $\mathbf{F}(t)$  (see Section II). These interference effects are analogous to multi-slit interference with the avoided crossings corresponding to the slits, and the time separating the avoided crossings to the slit spacing. From this perspective, twisted rapid passage with adjustable twist strength acts like a temporal interferometer which allows one to greatly enhance or suppress qubit transitions. Cubic and quartic twist were explicitly considered in this paper as they are, respectively, the simplest examples of odd-order and even-order polynomial twist in which these interference effects are expected to occur. We have seen that this interference mechanism can be used to pump qubit energy-levels, as well as to strongly quench qubit transitions during *non-adiabatic* twisted rapid passage. Although cubic twist proved to be more effective at pumping than quartic twist, quartic twist was found to be much more effective at quenching qubit transitions. As seen in Section IV, the degree to which this enhanced quenching can be realized is limited by how precisely the parameters  $(\eta_4, \tau_0, \lambda)$  can be controlled. It was seen that control to 5 significant figures was sufficient to allow execution of *non-adiabatic* NOT and CNOT operations while maintaining error probabilities below the accuracy threshold for fault-tolerant operation. The marriage of operational speed with reliability is a direct consequence of the destructive interference that is possible between the 3 avoided crossings that can arise during rapid passage with quartic twist.

Because of the fundamental significance of quantum CNOT gates to quantum computing and quantum error correction [10, 11, 12], it is hoped that the feasibility of using rapid pas-

### Transition Probability vs. Time

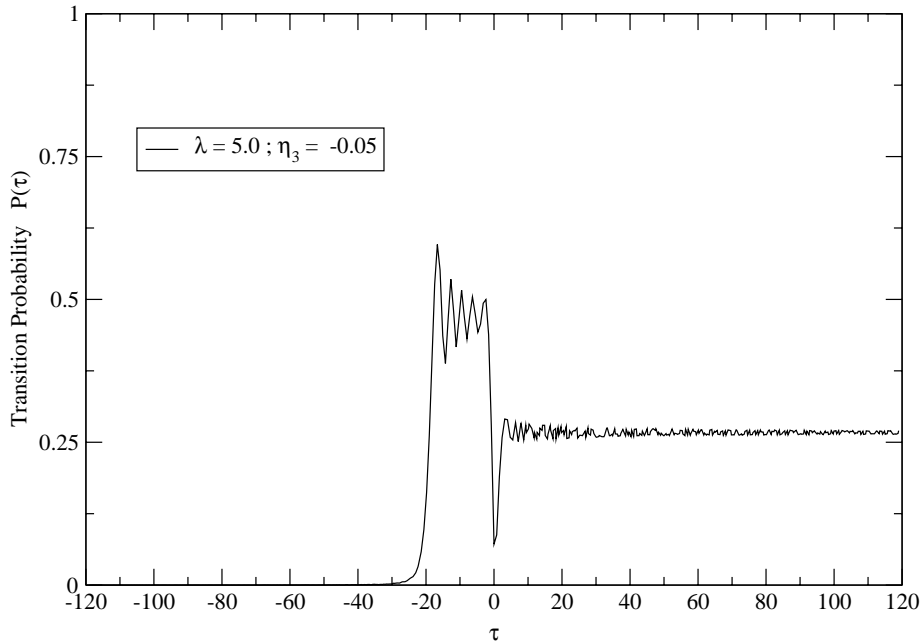


FIG. 8: The transition probability  $P(\tau)$  for non-adiabatic rapid passage with cubic twist with  $\lambda = 5.0$  and  $\eta_3 = -0.05$ .

sage with quartic twist to implement this gate might be tested experimentally. Experimental realization of polynomial twist  $\phi_n(t) = (2/n)Bt^n$  should be possible through an adaptation of the procedure used by Zwanziger et. al. [3] to realize quadratic twist. Thus: (1) the driving rf-field is linearly polarized along the x-axis in the lab-frame with  $F_x(t) = 2b \cos \phi_{rf}(t)$ ; (2) the resonance offset  $at$  (see eqn. (1)) is produced by linearly sweeping the detector frequency  $\omega_{det}(t)$  through the resonance at the Larmor frequency  $\omega_0$  such that  $\omega_{det}(t) = \omega_0 + (at/\hbar)$ ; and (3) twist is introduced by sweeping the rf-frequency  $\omega_{rf}(t) = \dot{\phi}_{rf}$  through the resonance at  $\omega_0$  in such a way that  $\omega_{rf}(t) = \omega_{det} - (\dot{\phi}_n/2)$ . It is worth noting that the resonance condition  $\omega_{rf}(t) = \omega_0$  is identical to our existence condition for avoided crossings, eqn. (5). Note that in our paper the external field inversion takes place over the time-interval  $(-T_0/2, T_0/2)$ ; the external field crosses the x-y plane at  $t = 0$  and is initially aligned along the  $-\hat{z}$  direction.

We hope in the future to examine higher order versions of polynomial twist to determine whether they have more effective quenching and/or robustness properties than cubic and quartic twist. We have also done preliminary work on the interesting case of periodic twist:  $\phi(t) = \pi\rho \sin \omega t$ . As we have seen, polynomial twist only allows 1–3 avoided crossings to occur during rapid passage. One can show that periodic twist allows the number of avoided crossings that occur during rapid passage to be modified through variation of the twist frequency  $\omega$ . We intend to explore how the interference effects considered here are modified when more than 3 avoided crossings can occur.

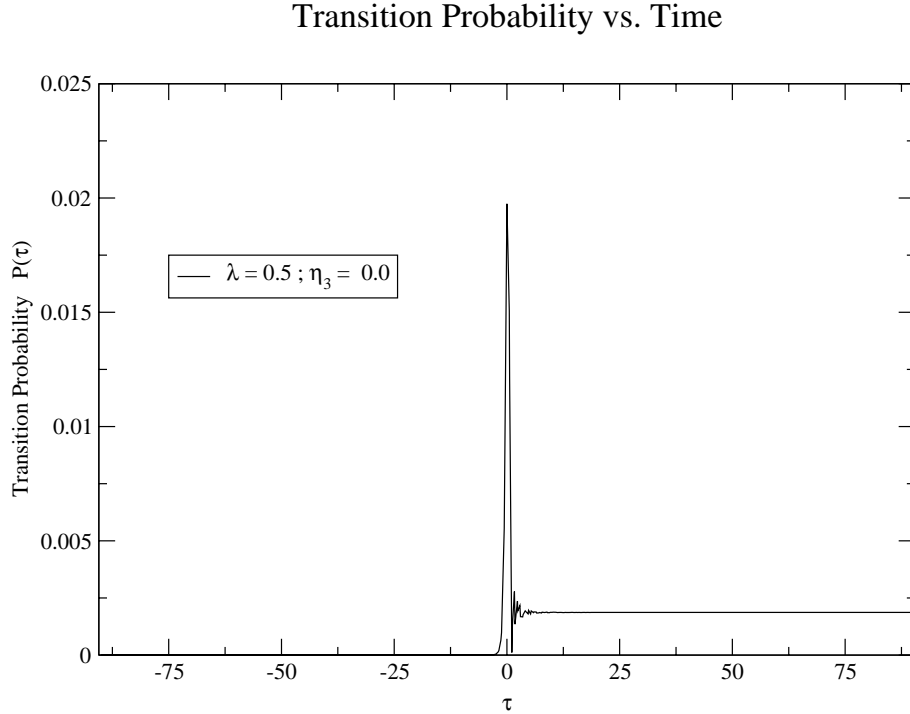


FIG. 9: The transition probability  $P(\tau)$  for twistless adiabatic rapid passage with  $\lambda = 0.5$  and  $\eta_3 = 0$ . Note the greatly reduced vertical scale compared to previous figures.

### Acknowledgments

I would like to thank: (1) T. Howell III for continued support; and (2) the National Science Foundation for support provided through grant number NSF-PHY-0112335.

- 
- [1] A. Abragam, *Principles of Nuclear Magnetism* (Oxford University Press, New York 1961).
  - [2] M. V. Berry, Proc. R. Soc. Lond. A **430**, 405 (1990).
  - [3] J. W. Zwanziger, S. P. Rucker, and G. C. Chingas, Phys. Rev. A **43**, 3232 (1991).
  - [4] L. Landau, Phys. Z. Sowjetunion **1**, 46 (1932)
  - [5] C. Zener, Proc. R. Soc. Lond. A **137**, 696 (1932).
  - [6] M. V. Berry, Proc. R. Soc. Lond. A **392**, 45 (1984).
  - [7] W. R. Thorson, J. B. Delos, and S. A. Boorstein, Phys. Rev. A **4**, 1052 (1971).
  - [8] The uncertainty in the average value of  $P$  is identified with the standard deviation of the 10 values of  $P$  used to determine the average transition probability. Note that when the uncertainty is less than the precision cited in the text for  $P$ , the uncertainty will be suppressed.
  - [9] P. Shor, in *Proceedings of the 37th Symposium on the Foundations of Computer Science*, (IEEE Computer Society Press, Los Alamitos, CA 1996), pp. 56-65; D. Gottesman, PhD thesis preprint <http://www.arxiv.org/quant-ph/9705052>; and J. Preskill, Proc. R. Soc. Lond. A **454**, 385 (1998).
  - [10] D. P. DiVincenzo, Proc. R. Soc. Lond. A **454**, 261 (1998).
  - [11] A. Barenco et. al. , Phys. Rev. A **52**, 3457 (1995).

### Transition Probability vs. Time

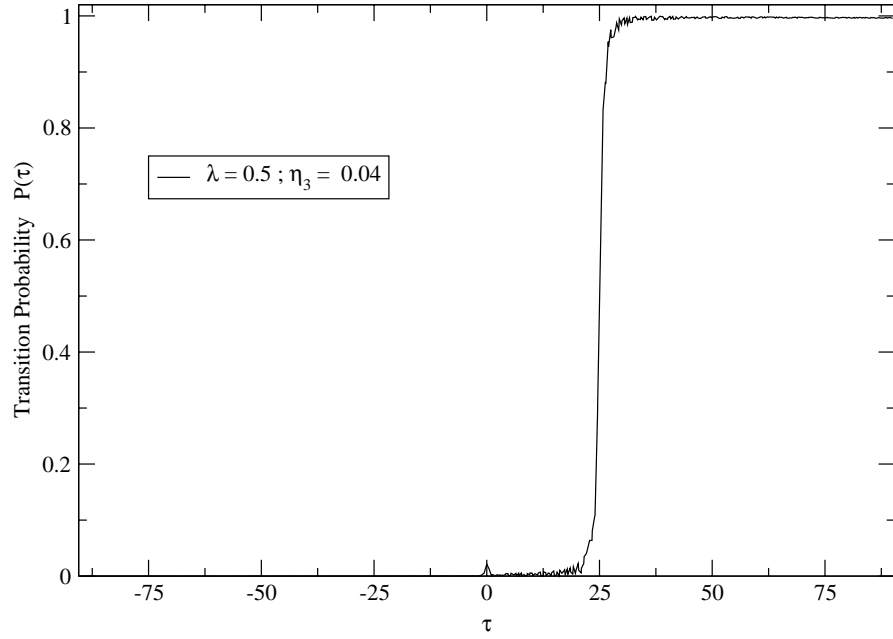


FIG. 10: The transition probability  $P(\tau)$  for adiabatic rapid passage with cubic twist with  $\lambda = 0.5$  and  $\eta_3 = 0.04$ .

- [12] P. W. Shor, Phys. Rev. A **52**, R2493 (1995); A. M. Steane, Proc. R. Soc. Lond. A **452**, 2551 (1996); A. R. Calderbank and P. W. Shor, Phys. Rev. A **54**, 1098 (1996); D. Gottesman, Phys. Rev. A **54**, 1862 (1996); E. Knill and R. Laflamme, Phys. Rev. A **55**, 900 (1997); see also A. M. Steane, in *Introduction to Quantum Computation and Information*, eds. H. K. Lo, S. Popescu, and T. Spiller (World Scientific, New Jersey, 1998).



### Transition Probability vs. Time

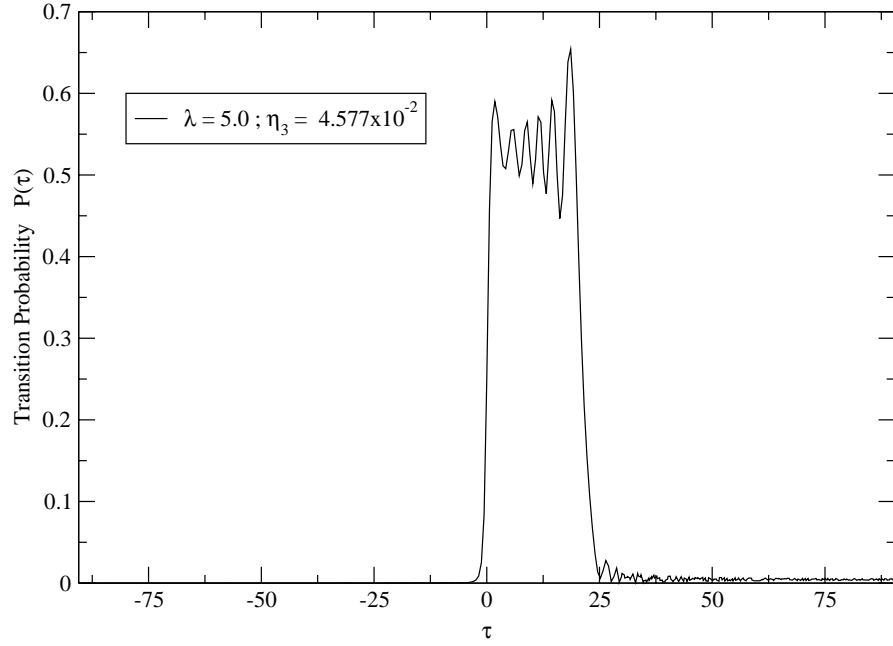


FIG. 11: The transition probability  $P(\tau)$  for non-adiabatic rapid passage with cubic twist with  $\lambda = 5.0$  and  $\eta_3 = 4.577 \times 10^{-2}$ . Note the slightly reduced vertical scale.

### Transition Probability vs. Time

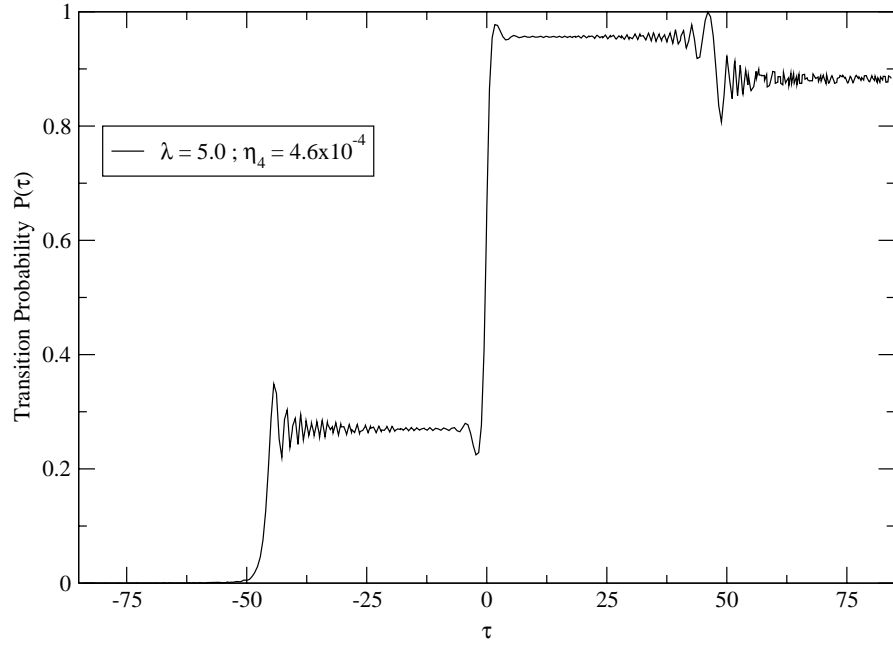


FIG. 12: The transition probability  $P(\tau)$  for non-adiabatic rapid passage with quartic twist with  $\lambda = 5.0$  and  $\eta_4 = 4.6 \times 10^{-4}$ .

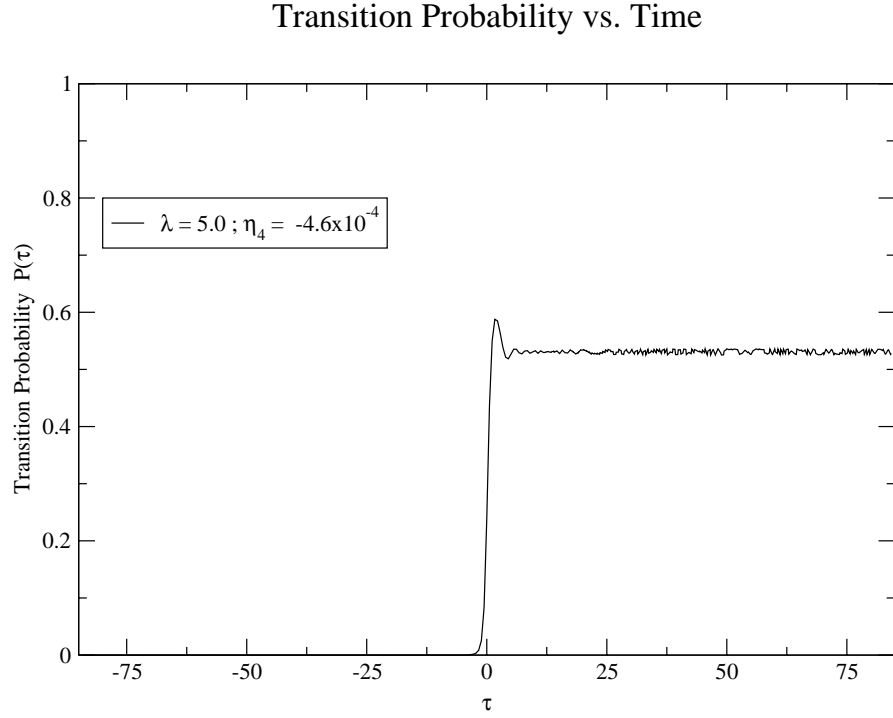


FIG. 13: The transition probability  $P(\tau)$  for non-adiabatic rapid passage with quartic twist with  $\lambda = 5.0$  and  $\eta_4 = -4.6 \times 10^{-4}$ .

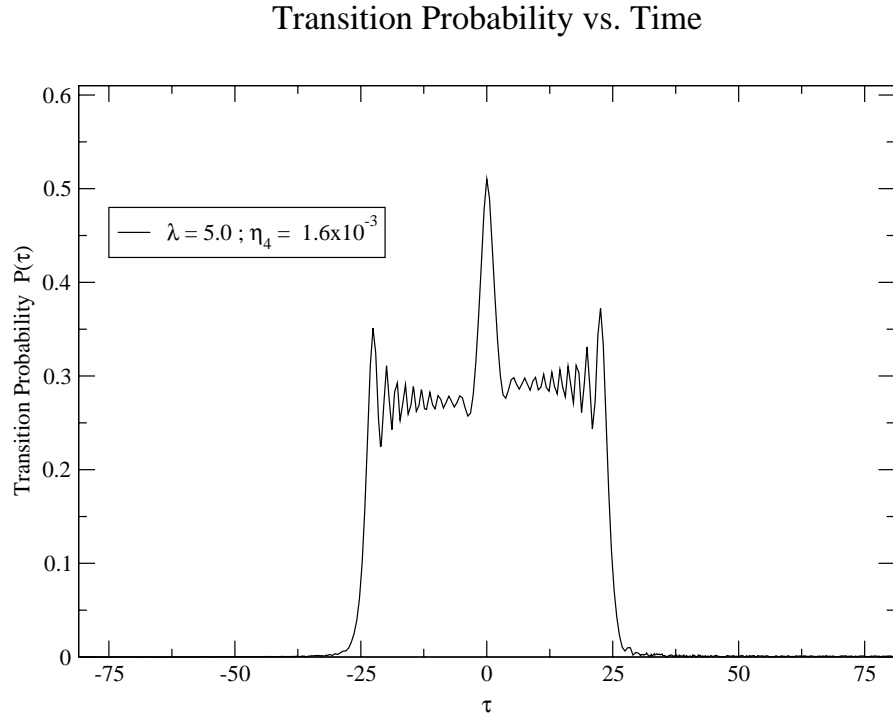


FIG. 14: The transition probability  $P(\tau)$  for non-adiabatic rapid passage with quartic twist with  $\lambda = 5.0$  and  $\eta_4 = 1.6 \times 10^{-3}$ . Note the slightly reduced vertical scale.

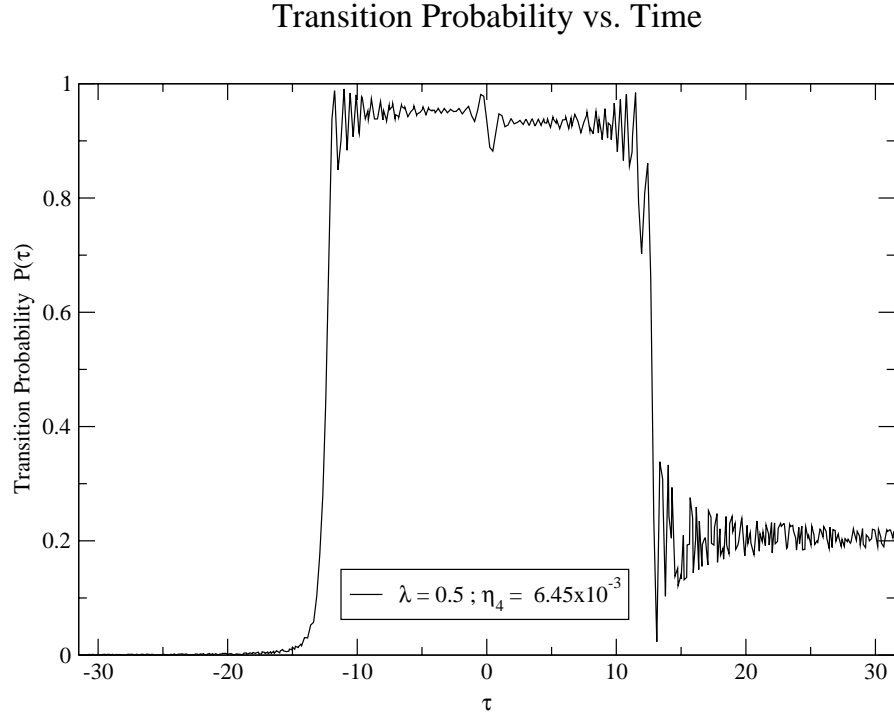


FIG. 15: The transition probability  $P(\tau)$  for adiabatic rapid passage with quartic twist with  $\lambda = 0.5$  and  $\eta_4 = 6.45 \times 10^{-3}$ .